# Crucial pathophysiological role of CXCR2 in experimental ulcerative colitis in mice

Pasquale Buanne,* Emma Di Carlo,[†,‡] Lorenzo Caputi,* Laura Brandolini,* Marco Mosca,* Franca Cattani,* Luigi Pellegrini,* Leda Biordi,[§] Gino Coletti,[¶] Carlo Sorrentino,[†,‡] Guido Fedele,[‖] Francesco Colotta,[*,#] Gabriella Melillo,* and Riccardo Bertini[*,1]

**Department of Preclinical Pharmacology, Dompé pha.r.ma s.p.a., L'Aquila, Italy; [†]Department of Oncology and Neurosciences, Surgical Pathology Section, "G. d'Annunzio" University, Chieti, Italy; [‡]Ce. S.I. Aging Research Center, "G. d'Annunzio" University Foundation, Chieti, Italy; [§]Experimental Medicine Department, University of L'Aquila, L'Aquila, Italy; [¶]Operative Unit of Pathological Anatomy, S. Salvatore Regional Hospital, L'Aquila, Italy; [‖]Biometry Unit, Dompé pha.r.ma s.p.a., Milan, Italy; and [#]Nerviano Medical Sciences, Milan, Italy*

**Abstract: Polymorphonuclear leukocyte infiltration and activation into colonic mucosa are believed to play a pivotal role in mediating tissue damage in human ulcerative colitis (UC). Ligands of human CXC chemokine receptor 1 and 2 (CXCR1/R2) are chemoattractants of PMN, and high levels were found in the mucosa of UC patients. To investigate the pathophysiological role played by CXCR2 in experimental UC, we induced chronic experimental colitis in WT and CXCR2$^{-/-}$ mice by two consecutive cycles of 4% dextran sulfate sodium administration in drinking water. In wild-type (WT) mice, the chronic relapsing of DSS-induced colitis was characterized by clinical signs and histopathological findings that closely resemble human disease. CXCR2$^{-/-}$ mice failed to show PMN infiltration into the mucosa and, consistently with a key role of PMN in mediating tissue damage in UC, showed limited signs of mucosal damage and reduced clinical symptoms. Our data demonstrate that CXCR2 plays a key pathophysiological role in experimental UC, suggesting that CXCR2 activation may represent a relevant pharmacological target for the design of novel pharmacological treatments in human UC. *J. Leukoc. Biol.* 82: 1239–1246; 2007.**

***Key Words:*** *rodent · neutrophils · inflammation*

## INTRODUCTION

Ulcerative colitis is a chronic inflammatory bowel disease (IBD), clinically characterized by frequent diarrheic attacks and anal bleeding. Histological hallmark of UC are the invasion of crypt epithelium and lamina propria by PMN, disruption of the epithelial lining, and, consequently, mucosal ulceration and crypt abscess formation in the bowel wall [1, 2]. PMN infiltration is believed to play a pivotal role in mediating tissue damage in UC. In animal studies an association between colonic neutrophilia and progression of acute colitis was observed [3, 4]. In humans, PMN accumulation has been observed in rectal biopsies of patients with active UC relative to healthy controls [5, 6].

Interleukin-8 (IL-8/CXCL8), a member of CXC chemokines, is a chemoattractant of PMN. Two high-affinity human CXCL8 receptors are known, CXC chemokine receptor 1 (CXCR1) and CXC chemokine receptor 2 (CXCR2). Although a mouse ortholog of CXCL8 has not been identified, the two corresponding receptors have been identified in the mouse [7, 8]. By recruiting and activating PMN, CXCL8 has been implicated in a wide range of disease states characterized by PMN infiltration in different organs [9], including UC [10]. CXCL8 is expressed in the colonic mucosa of patients affected by UC [11, 12] and IBD [13, 14] and a correlation between CXCL8 levels, PMN number in mucosal tissue, and the severity of UC has also been described [15, 16].

To investigate the pathophysiological role played by CXCR2 and its specific ligands in experimental UC, we induced chronic relapsing DSS-mediated colitis in WT and CXCR2$^{-/-}$ mice. Among animal models of UC, the chronic relapsing DSS-induced colitis resembles human UC under several features, including clinical symptoms and histopathological changes [17]. CXCR2$^{-/-}$ mice were reported to bear and develop normally, but their PMN were unable to migrate in response to its specific ligands CXCL1 (GROα/KC) and CXCL2 (GROβ/MIP-2) when compared with their WT littermates [18]. The results reported hereafter point out that the functional lacking of CXCR2 produced an amelioration of experimental UC, as shown by a significant improvement of clinical conditions paralleled by a reduction of the histopathological hallmarks of this disease model. These data are in keeping with a key role of CXCR2 in mediating PMN recruitment and tissue damage in experimental UC, suggesting that CXCR2 activation may represent a relevant pharmacological target for the design of novel pharmacological treatments in human UC.

[1] Correspondence: Department of Preclinical Pharmacology, Dompé pha.r.ma s.p.a., Via Campo di Pile 67100 L'Aquila, Italy. E-mail: bertini@dompe.it

Received February 19, 2007; revised March 28, 2007; accepted June 21, 2007.

doi: 10.1189/jlb.0207118

## MATERIALS AND METHODS

### Animals

Male, 6-wk-old BALB/c mice weighing 19-23 g were obtained from Charles River Laboratories (Calco, Lecco, Italy). Male CXCR2$^{-/-}$ mice on BALB/c background (strain C129S2 (B6)-IL8RB) were derived from founders provided by Jackson Laboratories (Bar Harbor, ME, USA) and genotyped by polymerase chain reaction (PCR) [19]. The animals were housed in cages up to five mice each and acclimated for 1 wk under conditions of controlled temperature (20°C±2), humidity (55%±10), and lighting (7:00 AM–7:00 PM). Sterilized diet No. 48 pellets (Laboratorio Dottori Piccioni, Gessate, Milan, Italy) and water were supplied ad libitum during acclimatization and experimental sessions.

All the procedures were performed in the animal operating rooms, according to ethical guidelines for the conduct of animal research (Authorization Italian Ministry of Health No. 50/2001-B; Italian Legislative Decree 116/92, Gazzetta Ufficiale della Repubblica Italiana No. 40, February 18, 1992; EEC Council Directive 86/609, OJL 358, 1, December 12, 1987; National Institutes of Health *Guide for the Care and Use of Laboratory Animals*, NIH Pub. No. 85-23, 1985).

### Chronic DSS colitis model

Chronic colitis was induced by 4% DSS (36–50 kDa, ICN Biochemicals, Milan, Italy) in drinking water in two consecutive cycles, as previously reported [20, 21]. The first DSS cycle was from day 0 to day 6. This cycle was followed by 14 days of simple ultrafiltered water (1st washout phase), from day 6 to day 20. The second DSS cycle (from day 20 to day 24) induced the relapse of the disease and was followed by three days of ultrafiltered water (2nd washout phase), from day 24 to day 27. Control group received water during all the experimental sessions. During the setup of the model, colitis was induced in Balb/c mice obtained from Charles River Laboratories and WT mice (CXCR2$^{+/+}$) derived from founders by Jackson Laboratories. No differences were seen in terms of clinical and histopathological response between the two inbred Balb/c strains. In all of the experiments reported hereafter, WT mice derived from founders by Jackson Laboratories were used.

### Clinical evaluation of DSS-induced colitis

Disease progression was determined at crucial time points by assessment of disease activity index (DAI), which ranged from 0 to 7. DAI score was calculated accordingly to previous reports [17, 22], adding two separate scores: Stool score (0=Normal; 1=>30% pellets with smooth consistency or <30% pellets with diarrheic consistency; 2=30–70% pellets with diarrheic consistency; 3=>70% pellets with diarrheic consistency) and Emo score (0=negative; 1=occult blood positive; 2=small blood drops on the pellet; 3=gross anal bleeding; 4=blood drops at the bottom of the cage). Occult blood in feces was determined by Hemo-fec (Roche Diagnostics, Mannheim, Germany).

### Histopathological, ultrastructural, immunohistochemical, and immunofluorescent analysis

Colon from the ileocecal valve to the anus was removed, washed in ice-cold saline, fixed in 10% neutral buffered formalin, embedded in paraffin and stained with hematoxylin and eosin. Histopathological score was assigned by two blinded pathologists. According to grading scales of histological assessment in human UC [23, 24], histopathological score was calculated as sum of single scores (ranged from 0 to 15), taking into account crypt distortion, loss of muco-secretive capability, percentage of severe ulcers, amount of inflammatory infiltrate in the severe ulcers expressed as granulocytes/severe ulcer thickness ratio (G/U ratio), and extension of tissue damage. The amount of inflammatory infiltrate in severe ulcers (expressed as G/U ratio) was singularly considered and defined as inflammatory score ranging from 0 to 5.

For electron microscopy, specimens were fixed in cacodylate buffered 2.5% glutaraldehyde, postfixed in osmium tetroxide and embedded in Epon 812. Ultrathin sections were stained with uranyl acetate-lead citrate.

For immunohistochemistry, large intestines were embedded in optimum cutting temperature compound (Miles), snap-frozen in liquid nitrogen and stored at −80°C. Then, frozen samples were sectioned, air dried overnight, fixed with acetone, and immunostained with anti-CXCL1 (Peprotech, Rocky Hill, NJ), anti-CD11c (Chemicon International, Temecula, CA, USA), anti-CD11b (Mac-1; Sera-Lab), anti-cytokeratins (CK) 8/18 (Progen Biotechnick, Heidelberg, Germany), anti-CD8 (Ly/T2; Sera-Lab), and anti-CD4 (LT34; Sera-Lab), anti-GR-1 (American Type Culture Collection) Abs. After washing, sections were overlaid with biotinylated goat anti-rat, anti-hamster, anti-rabbit and horse anti-goat Ig (Vector Laboratories, Burlingame, CA, USA). Unbound Ig was removed by washing, and slides were incubated with ABC (avidin/biotin complex)/alkaline phosphatase (DakoCytomation, Glostrup, Denmark).

For double immunofluorescent staining and confocal analysis, acetone-fixed frozen sections were incubated with the first primary antibodies and then with biotinylated secondary antibodies. After washing, sections were incubated with the second primary antibodies and, after washing, with biotinylated secondary antibodies and then with Alexa Fluor 594 conjugated StreptAvidin. Cross-reactions between the first secondary antibodies and Alexa Fluor 594 was prevented by saturation of all of its binding sites with Alexa Fluor 488. Slides were mounted with Vectashield medium (Vector Laboratories) and examined with a LSM 510 Meta laser scanning confocal microscope (Zeiss, Jena, Germany).

### Myeloperoxidase activity

Three centimeters of colon from anus were ice-homogenized (Ultra–Turrax, Ika-Werk) in a tube containing 1 ml/100 mg of tissue of 50 mM PBS, pH 6.0 and 0.5% HTAB (Sigma-Aldrich, St. Louis, MO, USA). Then samples were ice-sonicated (Ultrasonic processor XL) and ultracentrifuged (Sorvall RC5C) at 40,000 *g* at 4°C [25]. The supernatants were assayed for MPO activity [26]. Protein assay was performed by bicinchoninic acid method (Pierce Biotechnology, Rockford, IL, USA).

### CXCL1 and CXCL2 production

Three centimeters of colon from the anus were removed, ice-homogenized with protease inhibitors (5 μg/ml leupeptin, pepstatin, chimostatin, aprotinin and 1 mM PMSF; Sigma-Aldrich) and centrifuged at 20,800 *g* at 4°C (Centrifuge 5417 R, Eppendorf). Measurement of CXCL1 and CXCL2 was performed in the supernatants by using mouse CXCL1 and CXCL2 ELISA kits (R&D Systems, Minneapolis, MN, USA), according to manufacturer's instructions.

### Statistical analysis

Data are expressed as means ± SEM. All the analyses were conducted by using SAS 9,1 TS Level 1M3 in Windows XP professional environment.

DAI score was analyzed by Cochran-Mantel-Haenszel test (CMH) [27] and mixed linear models of analysis of variance (ANOVA) for repeated measures on data transformed by ranks [28]. Histopathological and inflammatory scores were processed by applying both Exact $\chi^2$-test or CMH and mixed linear models of ANOVA for a model completely random on data transformed by ranks. ANOVA followed by Dunnett's multiple comparison test was performed for CXCL1 and CXCL2 production data.

## RESULTS

### Lacking of CXCR2 reduces clinical signs in DSS-induced chronic colitis

The chronic relapsing DSS-induced colitis was induced by the administration of two cycles of DSS, with a washout period in between. In this model, as described previously [17, 22], the first 6-day cycle of DSS induced in WT mice an acute inflammation with a spontaneous gradual resolution when DSS administration was stopped.

To induce relapsing colitis, a second cycle of DSS administration was started at day 20 until day 24, as described previously [20]. DAI score increased in a time-dependent manner, reaching the maximum value at day 24 and persisting until day 27.

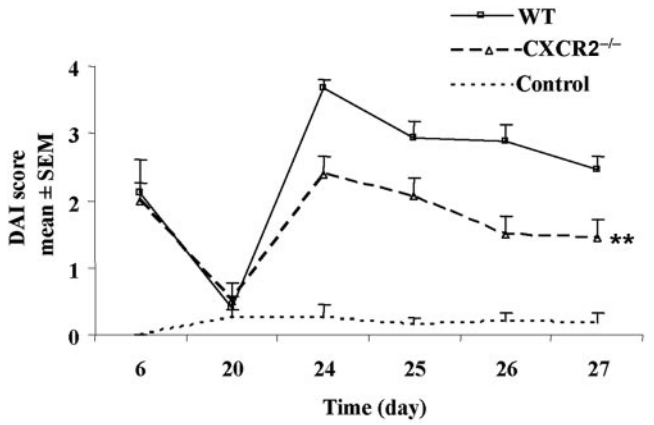


**Fig. 1.** Clinical evaluation of DSS-induced colitis in wild-type (WT) and CXC chemokine receptor 2 ($CXCR2^{-/-}$) mice. The clinical progression of the colitis was determined by disease activity index (DAI), calculated by adding two separate scores (ranging from 0 to 7): Stool score (0=normal; 1=>30% pellets with smooth consistency or <30% pellets with diarrheic consistency; 2=30–70% pellets with diarrheic consistency; 3=>70% pellets with diarrheic consistency) and Emo score (0=negative; 1=occult blood positive; 2=small blood drops on the pellet; 3=gross anal bleeding; 4=blood drops at the bottom of the cage). Colitis was induced in WT and $CXCR2^{-/-}$ mice by giving 4% DSS in drinking water in two cycles. Control group received water. Data are reported as means ± SEM (24–35 animals for each time point from one experiment of three). **, $P < 0.01$ vs. DSS-treated WT group by ANOVA.

To assess the role of CXCR2 in the chronic relapsing disease, DSS colitis was induced in $CXCR2^{-/-}$ mice. As shown in **Fig. 1**, the first cycle of DSS administration induced in $CXCR2^{-/-}$ mice a clinical outcome similar to WT mice (2.00 ± 0.51 and 2.11 ± 0.50 in $CXCR2^{-/-}$ and WT mice at day 6, respectively). DSS-second cycle caused a time-dependent increase in DSS-treated WT mice, reaching the maximum value at day 24. A significant reduction ($P<0.001$) of clinical signs of colitis (from 30% up to 48% of inhibition at day 24 and day 27, respectively) was observed in $CXCR2^{-/-}$ mice in comparison with WT. At day 27, the time of sacrifice, the DAI score of $CXCR2^{-/-}$ group was 42% lower than that of WT group (1.44 ± 0.22 and 2.47 ± 0.19 in $CXCR2^{-/-}$ and WT mice, respectively) (Fig. 1). The clinical score improvement observed in $CXCR2^{-/-}$ mice was evident both as stool consistency and as blood in feces.

## Reduction of colonic mucosa damage in $CXCR2^{-/-}$ mice

To gain insights into the cellular mechanisms underlying the reduced severity of experimental colitis in $CXCR2^{-/-}$ mice, we carried out a histopathological analysis of gut lesions induced in both $CXCR2^{-/-}$ and WT mice. The histopathological analysis included both nonspecific gut lesions (e.g., crypt distortion) and inflammatory-specific lesions (e.g., severe ulcer formation).

According to previous reports [17, 22], the first cycle of DSS administration induced a pathological status with a low involvement of inflammatory cells and reduced tissue damage. Only few PMN, lymphocytes, and plasma cells, incoming from submucosa, were detected between crypts and into crypt epithelium. Initial erosions were also observed but without PMN stratifications (data not shown).

During the second DSS cycle, clinical symptoms (see above) were related by progressive histopathological changes, characterized by a dramatic infiltration of PMN from the lamina propria into the colonic mucosa causing severe ulcers **(Fig. 2C–E)** and microabscesses formation (Fig. 2F). No histopathological change was reported in control group (Fig. 2A, B). As shown in **Fig. 3**, massive PMN recruitment into colonic segment was further confirmed by increased tissue MPO, a well-known specific marker of PMN (5.81 ± 0.11 and 171.25 ± 12.16 mU/mg protein in water and DSS-treated WT mice at day 27, respectively). Large tracts of mucosa lost the epithelium

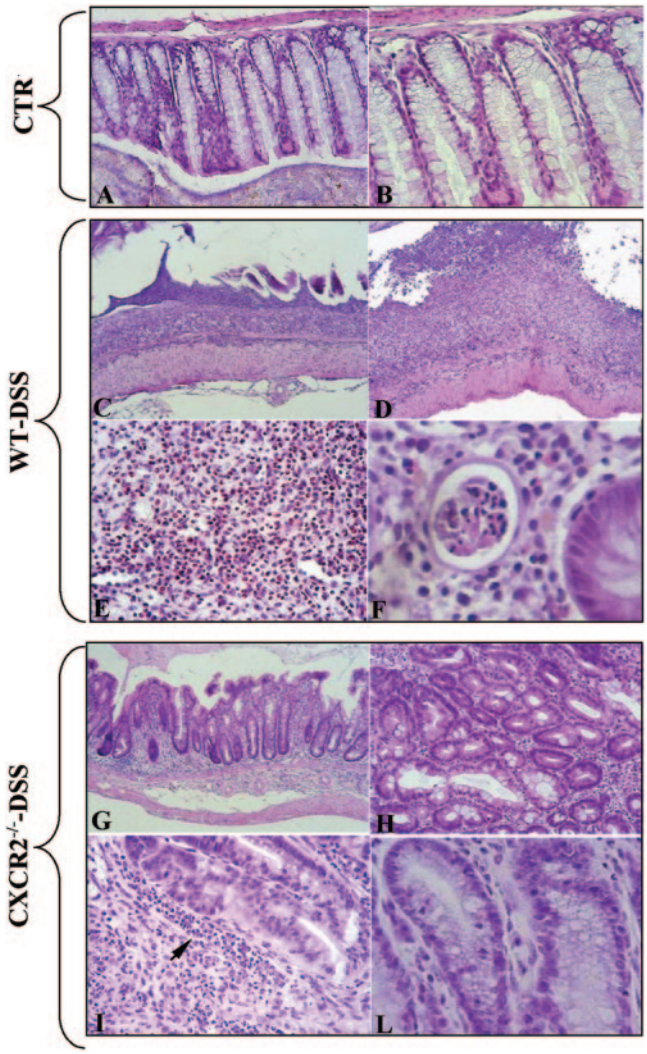


**Fig. 2.** Histopathological analysis of DSS-induced colitis in WT and $CXCR2^{-/-}$ mice. Colon from the ileocecal valve to the anus was removed and stained with hematoxylin and eosin. (A) and (B) control mice. At day 27, DSS induced massive infiltration of PMN into the crypt epithelial layer with necrosis and ulcerative lesions of colonic mucosa (C), (D), large tracts of mucosa lost crypt epithelium appeared to be replaced by granulation tissue (E) associated with a dramatic infiltration of PMN, causing microabscesses formation (F) in WT mice. The overall aspect of colonic mucosa was less severe in $CXCR2^{-/-}$ mice. A significant decrease of PMN aggregates was associated with a reduction of severe ulcers formation (G), (H). The inflammatory cells (indicated by arrow) were mainly confined into microvascular space, confined around the crypts (I). Muco-secretive ability preserved in $CXCR2^{-/-}$ mice (G), (H), (L). Original magnification, ×100 (A), (C), (D),(G); ×200 (B), (H); ×400 (E), (I), (L); ×1000 (F).

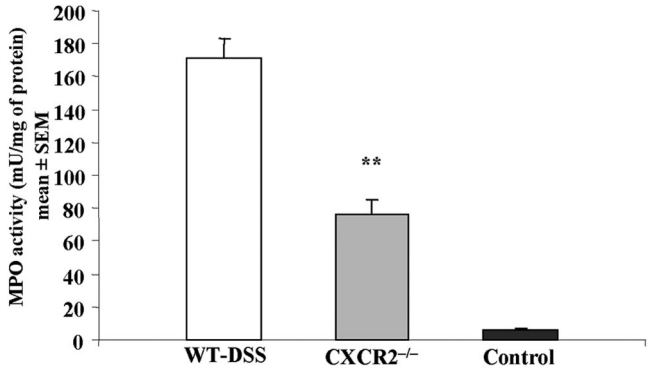


**Fig. 3.** MPO activity in the colon of DSS-treated WT and CXCR2$^{-/-}$ mice. WT and CXCR2$^{-/-}$ mice were killed at day 27 after DSS administration, and colonic mucosa were processed for determination of MPO activity. Control group received normal water. (**, $P<0.01$ vs. DSS-treated WT group by ANOVA). Data are expressed as mean ± SEM (14 animals for each experimental group from one experiment of three).

and was replaced by granulation tissue (Fig. 2E). The overall histopathological and inflammatory scores peaked at day 27 (**Fig. 4A, B**).

When CXCR2$^{-/-}$ mice were examined at day 27, DSS-treated CXCR2$^{-/-}$ mice showed PMN accumulation in the lumen of blood vessels and only limited extravasation and infiltration into the tissue. The few infiltrating PMN remained in close proximity of microvasculature, confined around the crypts and rarely penetrated the basal membrane, (Fig. 2I; 5C, E; and 6C–D) whereas in DSS-treated WT mice, PMN infiltrated the crypt epithelial layer, reaching tight contact with epithelial crypts thus causing necrotic and ulcerative lesions in colonic mucosa (**Fig. 5B, D** and **Fig. 6A, B**). In addition to neutrophils, also eosinophils infiltrate largely the mucosa of DSS-treated WT mice (Fig. 6A, B). These data are in keeping with previous descriptions of DSS-induced chronic colitis in the mouse [17, 29]. As shown in Fig. 3, reduction of PMN infiltration in CXCR2$^{-/-}$ mice was also confirmed by a significant ($P < 0.01$) reduction of mucosal MPO activity (171.25 ± 12.16 and 76.61 ± 8.42 mU/mg of protein in WT and CXCR2$^{-/-}$ mice, respectively). Areas of the mucosa retaining muco-secretive properties (maintenance of goblet cells) were, unlike WT counterparts (Fig. 2C–E), evident in CXCR2$^{-/-}$ mice (Fig. 2G–H and 2L). However, the presence of mitotic figures and "pseudo-stratification" of the crypt epithelium were observed in CXCR2$^{-/-}$ mice, providing evidence of the insult and the following regenerative process (Fig. 2L). Moreover, in CXCR2$^{-/-}$ mice, a significant decrease in the number of severe ulcers was observed (Fig. 2G). The overall histopathological and inflammatory scores were significantly reduced in CXCR2$^{-/-}$ mice at day 27 (53% and 56% of reduction, respectively) (Fig. 4A, B). At day 20, starting time of second cycle of DSS, no significant differences between WT and

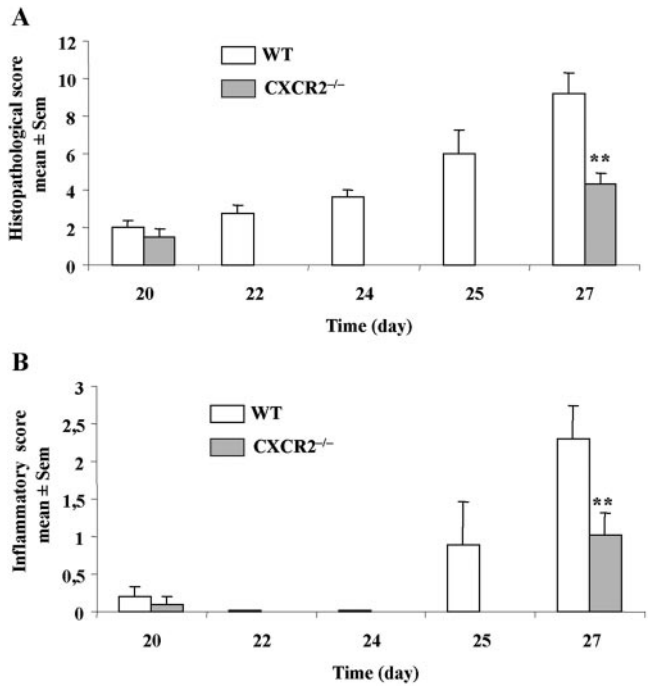


**Fig. 4.** Histopathological and inflammatory scores in DSS-treated WT and CXCR2$^{-/-}$ mice. Animals were killed during the chronic phase of DSS-induced colitis, and histopathological analysis was performed in the tract of the colon mainly involved by disease. (A) Histopathological score in CXCR2$^{-/-}$ and WT mice (**, $P < 0.01$ vs. DSS-treated WT group by ANOVA). (B) Inflammatory score in CXCR2$^{-/-}$ and WT mice (**, $P<0.01$ vs. DSS-treated WT group by ANOVA). Data are expressed as means ± SEM (14–25 animals for each time point from one experiment of three).

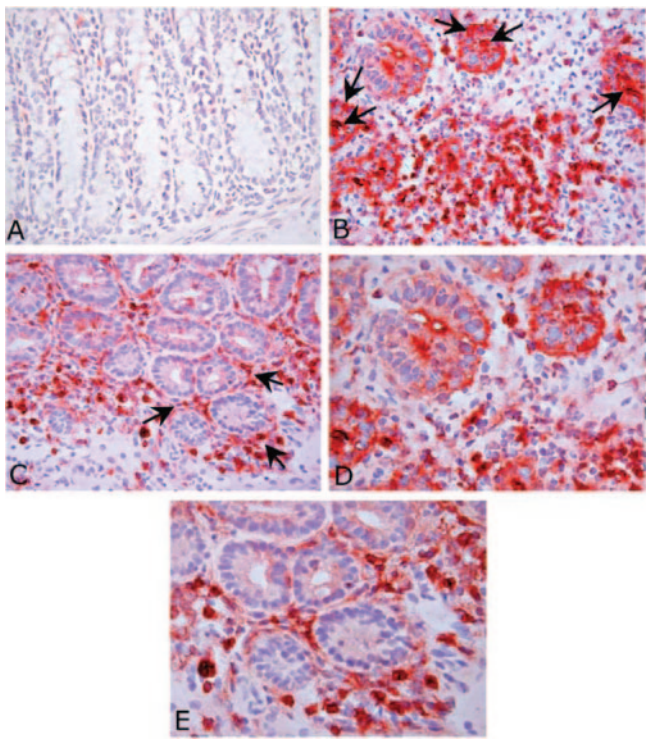


**Fig. 5.** Immunohistochemical analysis of colon section from WT and CXCR2$^{-/-}$ mice. Immunohistochemistry on intestinal sections from mice exposed to normal water or two cycles of DSS and killed at day 27. (A) Control (water-treated) WT animals. (B) DSS-treated WT mice. PMN infiltrated (arrows) and destroyed the crypt epithelial layer. (C) DSS-treated CXCR2$^{-/-}$ mice. PMN were mostly confined among the crypts (arrows). (D) DSS-treated WT mice. Magnification of details indicated by arrows in (B). (E) DSS-treated CXCR2$^{-/-}$ mice. Magnification of details indicated by arrows in (C). Original magnification, ×400.

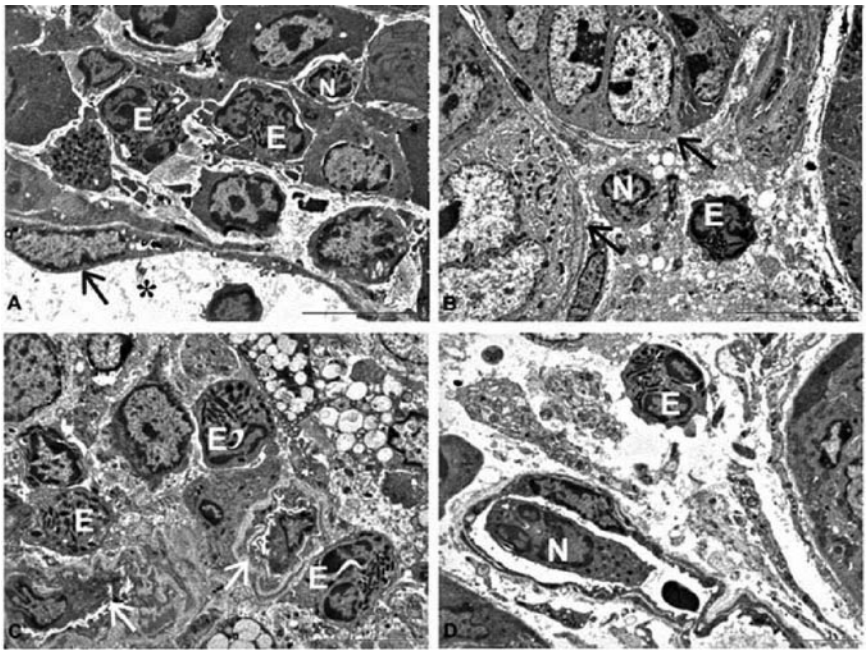


**Fig. 6.** Ultrastructural features of colonic lamina propria from DSS-induced chronic colitis in WT and CXCR2$^{-/-}$ mice. Colon sections from WT and CXCR2$^{-/-}$ mice killed at day 27 after DSS administration. (A, B) WT mice. In the colonic lamina propria, both eosinophils (E) and neutrophils (N) largely extravasated. Endothelial cells are indicated by arrow; vessel lumen indicated by asterisk. Eosinophils and neutrophils spread to the stroma, reaching tight contact with epithelial crypts (indicated by arrows). (C, D) CXCR2$^{-/-}$ mice. PMN extravasated in the colonic lamina propria but did not migrate, remaining in close proximity to microvessel walls (indicated by arrows). PMN stopped and filled microvessels. Bars in A and B = 100 μm. Bars in C and D = 50 μm.

CXCR2$^{-/-}$ mice were observed. However, in both experimental groups, there was an increase over baseline of histopathological and inflammatory scores in comparison with control group (Fig. 4A, B), indicating that a few histopathological signs of the insult still remained, even though they were not clinically detectable.

Thus, whereas WT mice develop a chronic colitis characterized by massive PMN infiltration and mucosal erosion, CXCR2$^{-/-}$ mice show no PMN infiltration into the mucosa and limited signs of mucosal damage, confirming the key role of PMN in mediating tissue injury in colitis.

## Time-dependent increase of production of CXCR2 ligands in DSS-treated WT

To further evaluate the different clinical and histopathological course of colitis in WT vs. CXCR2$^{-/-}$ mice, we examined the expression of CXCR2 ligands into colonic mucosa after DSS administration in both WT and CXCR2$^{-/-}$ mice. As shown in **Fig. 7A**, CXCL1 expression was almost absent in water-treated WT mice. During the chronic colitis, CXCL1 was consistently expressed in WT mice, peaking at day 27 (13.96±1.73 pg/mg of tissue). CXCL1 mucosal production was further confirmed by confocal microscopy (**Fig. 8**). CXCL1 was found to be expressed in the stroma of the lamina propria, especially close to the areas of PMN recruitment (Fig. 8A), mainly by (CD11c$^{+}$) dendritic cells (Fig. 8C) and (CD11b$^{+}$) macrophages to a lesser extent (Fig. 8D), whereas epithelial cells of the intestinal crypts were mostly negative (Fig. 8B). Also CXCL2 was consistently expressed in WT mice, with CXCL2 levels peaking again at day 27 (0.03±0.00 and 6.89±2.16 pg/mg of tissue in water-treated and DSS-treated animals, respectively (Fig. 7B).

When CXCR2$^{-/-}$ mice exposed to DSS were examined, we found that the CXCR2 ligand CXCL1 was expressed in the gut mucosa at levels similar to WT mice (e.g., 13.96±1.73 and 15.91 ± 1.13 pg/mg of tissue at day 27 in WT and CXCR2$^{-/-}$

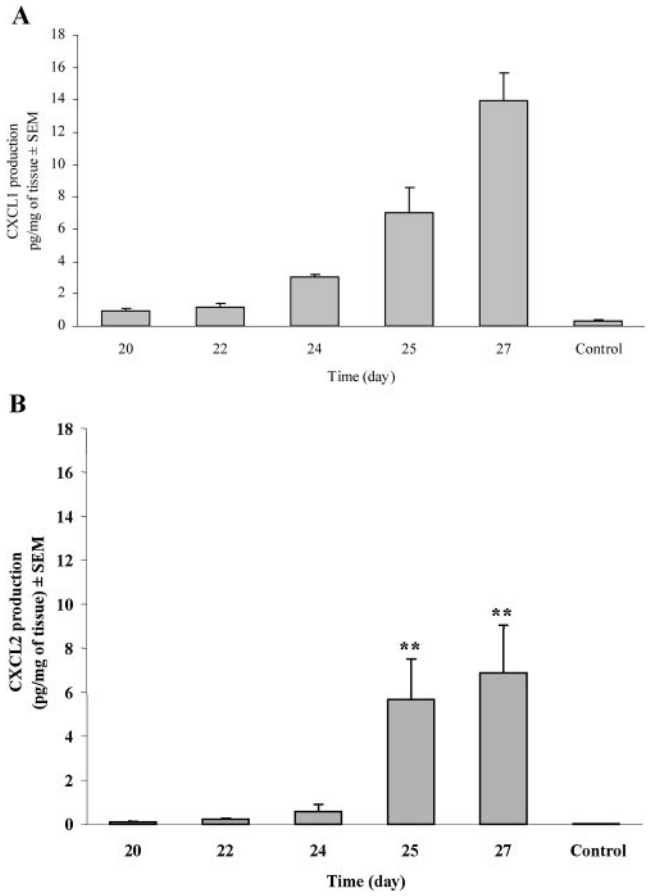


**Fig. 7.** Expression of CXCL1 and CXCL2 in the colon of DSS-treated WT mice. WT mice were killed after different times of DSS administration, and colonic mucosa was processed for CXCL1 and CXCL2 detection. Control group received normal water. (A) Colonic production of CXCL1 (**, $P<0.01$ vs. control group by ANOVA). (B) Colonic production of CXCL2 (**, $P<0.01$ vs. control group by ANOVA). Data are expressed as means ± SEM (14 animals for each time point).

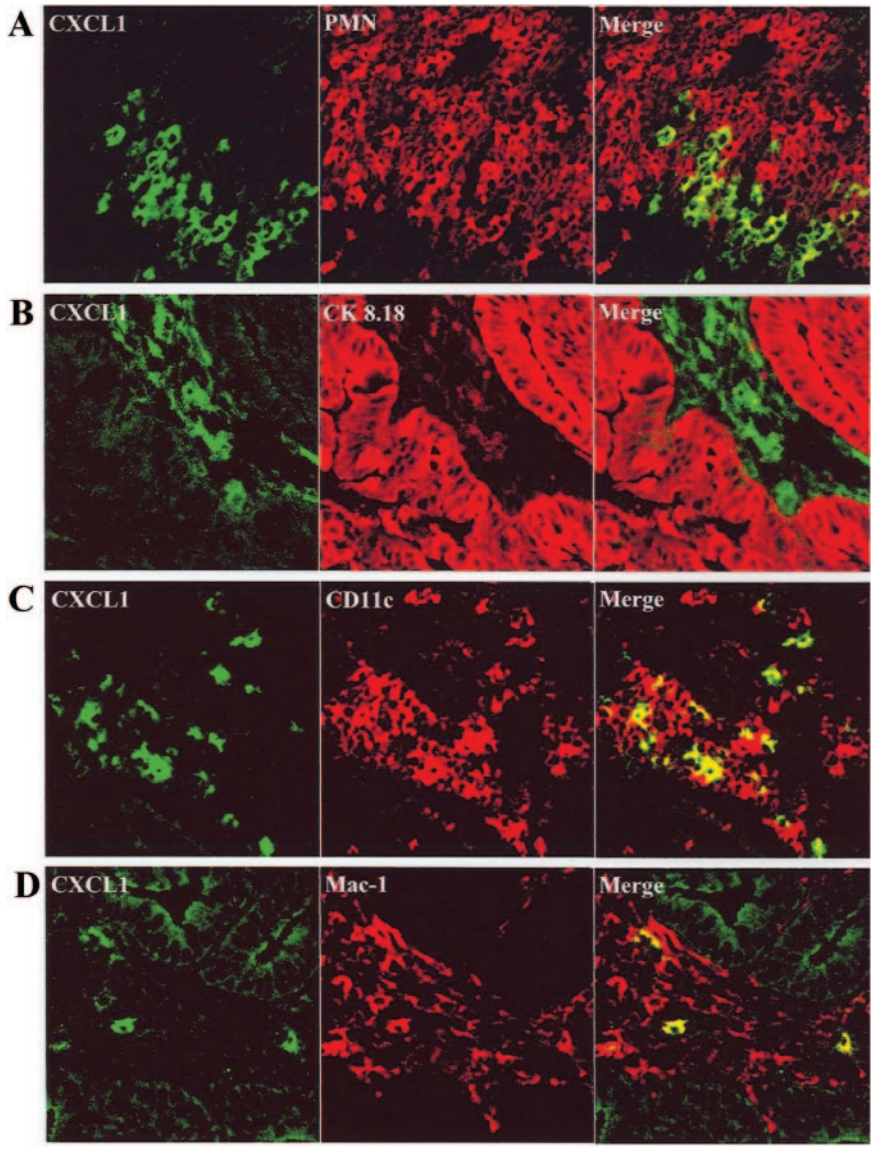


**Fig. 8.** Confocal analysis of CXCL1 expression in colonic mucosa of DSS-treated WT mice. Colon sections from WT mice exposed to two cycles of DSS and killed at day 27. (A) Massive influx of PMN (red stained) close to the mucosal areas rich in CXCL1 expression (green stained) without aspects of colocalization, as shown by the merge image. (B) Expression of CXCL1 (green stained) was mainly among the intestinal epithelial (red stained) crypts. (C) Most of dendritic cells (CD11c, red stained) infiltrating the lamina propria produce CXCL1 (green stained), as revealed by the yellow color in the merge image. (D) Macrophages (CD11b, red stained) infiltrating the lamina propria cooperate to CXCL1 production (green stained), as revealed by the yellow color in the merge image. Original magnification, ×400.

mice, respectively). An analogous result was observed for CXCL2 colonic expression (e.g., 5.24±4.42 and 2.58±1.25 pg/mg of tissue at day 27 in WT and CXCR2$^{-/-}$ mice, respectively).

## DISCUSSION

The infiltration of PMN into the colonic mucosa is believed to play a key role in mediating tissue damage and clinical symptoms in both human and experimental UC. We demonstrate here that PMN infiltration in the model of chronic colitis is mainly mediated by CXCR2. CXCR2$^{-/-}$ mice have limited, if any, PMN infiltration into the colonic mucosa in the relapsing phase of the disease. Accordingly with a key role played by PMN in mediating tissue damage in colitis, histopathologically detected mucosal damage, including mucosal ulcerations, and clinical signs were reduced in mice lacking a functional CXCR2.

Ligands of CXCR2 were expressed at high levels in experimental colitis of both WT and CXCR2$^{-/-}$ mice, and their production was strongly related to the increase of PMN recruitment into colonic mucosa of WT mice.

To assess the role of CXCR2, we used a model of DSS-induced colitis that closely resembles human UC under several features [30, 31]. In this model, repeated DSS administration induced epithelial atrophy, extensive loss of mucus production, widespread hyperplasia in large areas of the colonic mucosa, complete loss of crypt epithelium in large tract of mucosa, crypt abscesses, severe ulcers and, most notably, a massive infiltration of PMN into colonic mucosa. Also, from the clinical point of view, morphological changes observed after chronic administration of DSS were paralleled by clinical symptoms induced by repeated DSS administration that closely resemble severe human UC, including diarrhea and gross rectal bleeding [30]. Moreover, selected drugs currently used in the therapy of UC are also efficacious in this model of repeated DSS administration, including cyclosporin A [32] and infliximab [21, 33], a monoclonal antibody anti-TNF-α [34–36], further suggesting that the DSS model we used closely resembles the human condition.

In the DSS-induced colitis, both high levels of CXCR2 ligands and a massive recruitment of PMN were evident in WT mice during the chronic phase of disease.

The main histopathological changes and clinical symptoms in the DSS-induced experimental colitis were strongly reduced in $CXCR2^{-/-}$ mice. Lack of functional CXCR2 prevented PMN infiltration in the mucosa, suggesting that PMN recruitment into the gut mucosa is mainly attributable to CXCR2 activation. Inhibition of PMN recruitment was associated with a strong reduction in all histopathological changes associated with experimental colitis, including necrotic and ulcerative lesions in the colonic mucosa. Large areas of mucosa with intact muco-secretive properties were also observed in $CXCR2^{-/-}$ mice, whereas in WT mice, there was a strong reduction of mucus production, and large tracts of mucosa lost all crypt epithelium, leaving in its place granulation tissue. These data are further in keeping with the concept that PMN recruitment and activation in UC are key events in inducing mucosal damage and clinical symptoms. This evidence was apparently in contrast to a previous report [37], in which the abrogation of PMN has a deleterious effect on DSS-induced colitis. However, these results are referred to a single cycle of DSS administration, an experimental condition that does not resemble UC condition. Indeed, a single cycle of DSS administration induces a pathological state, with a low involvement of inflammatory cells and reduced tissue damage, mainly caused by the toxic effect of DSS on colonic epithelial cells [17, 22]. In addition, the efficacy of treatment with a monoclonal antibody anti-TNF-α and corticosteroids clinically proved in UC was not experimentally observed after a single cycle of DSS [38].

Whereas intraepithelial infiltration of PMN seems to be mediated mainly by CXCR2, we found that lack of CXCR2 has no effect on intravascular accumulation of leukocytes. These findings suggest that intravascular leukocyte recruitment might be under the control of other leukocyte-activating factors, such as TNF-α [20] and products of the complement system [39]. On the other hand, the impairment of PMN to cross endothelial surface and subsequently infiltration into the crypt epithelial barrier strongly suggest that PMN recruitment into the mucosa could be mainly dependent upon CXCR2 activity on endothelial and epithelial cells. In keeping with this hypothesis, several reports support the crucial role played by CXCR1 and CXCR2 activity on endothelial and epithelial cell layer in chemokine-mediated PMN arrest and subsequent transmigration into inflamed tissue [40–43]. Indeed, PMN of $CXCR2^{-/-}$ mice were unable to cross the epithelial barrier and accumulate in the tissue in an experimental model of infection of the urinary tract [42], and immunoneutralization of CXCL1 and CXCL2 did not reduce endotoxin-induced leukocyte intravascular accumulation, whereas PMN transmigration and extravascular tissue accumulation was abolished [40]. Similarly, CXCR1 and CXCR2 overexpression was detected in infected human uroepithelial cell lines, and neutralization of CXCR1 strongly inhibited CXCL8-dependent PMN migration across the epithelial cell layer [42]. Finally, the crucial role of CXCR2 for transendothelial and transepithelial migration of PMN, but not for their accumulation in the vasculature, was also reported in a murine model of acute lung injury in which PMN of $CXCR2^{-/-}$ mice did not migrate into the lung interstitium following endotoxin aerosolization, remaining into the pulmonary vasculature without inducing lung damage [44].

Although PMN infiltration is believed to be a key event in DSS-induced colitis, information as to the soluble factors involved in the regulation of PMN recruitment in this model are scanty. Here, we demonstrate that CXCR2 ligands (CXCL1 and CXCL2) are highly expressed in the stroma of the lamina propria, close to the areas of PMN recruitment. Production of these PMN attractants was mainly attributable to mononuclear and dendritic cells in the colonic mucosa. High levels of both CXCR1/R2 expression and CXCR1/2 ligands have also been found in the mucosa of UC patients [45].

Taken together, these findings demonstrate that CXCR2 plays a key, nonredundant role in mediating PMN infiltration into the mucosa in an animal model of colitis that closely resembles human UC. Prevention of PMN infiltration was associated with a strong reduction in both histopathological signs of the disease and clinical symptoms. These data may provide the rationale for testing CXCL8 receptors inhibitors as a new therapeutic approach to UC in the clinic.

## REFERENCES


1. Ajuebor, M. N., Swain, M. G. (2002) Role of chemokines and chemokine receptors in the gastrointestinal tract. *Immunology* **105,** 137–143.
2. Podolsky, D. K. (2002) Inflammatory bowel disease. *N. Engl. J. Med.* **347,** 417–429.
3. Palmen, M. J., Dijkstra, C. D., van der Ende, M. B., Pena, A. S., van Rees, E. P. (1995) Anti-CD11b/CD18 antibodies reduce inflammation in acute colitis in rats. *Clin. Exp. Immunol.* **101,** 351–356.
4. Natsui, M., Kawasaki, K., Takizawa, H., Hayashi, S. I., Matsuda, Y., Sugimura, K., Seki, K., Narisawa, R., Sendo, F., Asakura, H. (1997) Selective depletion of neutrophils by a monoclonal antibody, RP-3, suppresses dextran sulphate sodium-induced colitis in rats. *J. Gastroenterol. Hepatol.* **12,** 801–808.
5. Mazzucchelli, L., Hauser, C., Zgraggen, K., Wagner, H., Hess, M., Laissue, J. A., Mueller, C. (1994) Expression of interleukin-8 gene in inflammatory bowel disease is related to the histological grade of active inflammation. *Am. J. Pathol.* **144,** 997–1007.
6. Uguccioni, M., Gionchetti, P., Robbiani, D. F., Rizzello, F., Peruzzo, S., Campieri, M., Baggiolini, M. (1999) Increased expression of IP-10, IL-8, MCP-1, and MCP-3 in ulcerative colitis. *Am. J. Pathol.* **155,** 331–336.
7. Fan, X., Patera, A. C., Pong-Kennedy, A., Deno, G., Gonsiorek, W., Mandra, J. D., Vassileva, G., Zeng, A., Jackson, C., et al. (2006) Murine CXCR1 is a functional receptor for GCP-2/CXCL6 and IL-8/ CXCL8. *J. Biol. Chem.*, In press.
8. Lee, J., Cacalano, G., Camerato, T., Toy, K., Moore, M. W., Wood, W. I. (1995) Chemokine binding and activities mediated by the mouse IL-8 receptor. *J. Immunol.* **155,** 2158–2164.
9. Gerard, C., Rollins, B. J. (2001) Chemokine and disease. *Nat. Immunol.* **2,** 108–115.
10. Keshavarzian, A., Fusunyan, R. D., Jacyno, M., Winship, D., MacDermott, R. P., Sanderson, I. R. (1999) Increased interleukin-8 (IL-8) in rectal dialysate from patients with ulcerative colitis: evidence for a biological role for IL-8 in inflammation of the colon. *Am. J. Gastroenterol.* **94,** 704–712.
11. Banks, C., Bateman, A., Payne, R., Johnson, P., Sheron, N. (2003) Chemokine expression in IBD. Mucosal chemokine expression is unselectively increased in both ulcerative colitis and Crohn's disease. *J. Pathol.* **199,** 28–35.
12. Katsuta, T., Lim, C., Shimoda, K., Shibuta, K., Mitra, P., Banner, B. F., Mori, M., Bernard, G. F. (2000) Interleukin-8 and SDF1-alpha mRNA expression in colonic biopsies from patients with inflammatory bowel disease. *Am. J. Gastroenterol.* **95,** 3157–3164.
13. McCormack, G., Moriarty, D., O'Donoghue, D. P., McCormick, P. A., Sheahan, K., Baird, A. W. (2001) Tissue cytokine and chemokine expression in inflammatory bowel disease. *Inflamm. Res.* **50,** 491–495.

14. Daig, R., Andus, T., Aschenbrenner, E., Falk, W., Schölmerich, J., Gross, V. (1996) Increased interleukin-8 expression in the colon mucosa of patients with inflammatory bowel disease. *Gut* **38,** 216–222.
15. Izzo, R. S., Witkon, K., Chen, A. I., Hadjiyane, C., Weinstein, M. I., Pellecchia, C. (1992) Interleukin-8 and neutrophils markers in colonic mucosa from patients with ulcerative colitis. *Am. J. Gastroenterol.* **87,** 1447–1452.
16. Mitsuyama, K., Toyonaga, A., Sasaki, E., Watanabe, K., Tateishi, H., Nishiyama, T., Saiki, T., Ikeda, H., Tsuruta, O., Tanikawa, K. (1994) IL-8 as an important chemoattractant for neutrophils in ulcerative colitis and Crohn's disease. *Clin. Exp. Immunol.* **96,** 432–436.
17. Cooper, H. S., Murphy, S. N., Shah, R. S., Sedergran, D. J. (1993) Clinicopathologic study of dextran sulfate sodium experimental murine colitis. *Lab. Invest.* **69,** 238–249.
18. Cacalano, G., Lee, J., Kikly, K., Ryan, A. M., Pitts-Meek, S., Hultgren, B., Wood, W. I., Moore, M. W. (1994) Neutrophil and B cell expansion in mice that lack the murine IL-8 receptor homolog. *Science* **265,** 682–684.
19. Del Rio, L., Bennouna, S., Salinas, J., Denkers, E. Y. (2001) CXCR2 deficiency confers impaired neutrophil recruitment and increased susceptibility during *Toxoplasma gondii* infection. *J. Immunol.* **167,** 6503–6509.
20. Myers, K. J., Murthy, S., Flanigan, A., Witchell, D. R., Butler, M., Murray, S., Siwkowski, A., Goodfellow, D., Madsen, K., Baker, B. (2003) Antisense oligonucleotide blockade of tumor necrosis factor-alpha in two murine models of colitis. *J. Pharmacol. Exp. Ther.* **304,** 411–424.
21. Murthy, S., Flanigan, A., Coppola, D., Buelow, R. (2002) RDP58, a locally active TNF-α inhibitor, is effective in the dextran sulphate mouse model of chronic colitis. *Inflamm. Res.* **51,** 522–531.
22. Okayasu, I., Hatakeyama, S., Yamada, M., Ohkusa, T., Inagaki, Y., Nakaya, R. (1990) A novel method in the induction of reliable experimental acute and chronic ulcerative colitis in mice. *Gastroenterology* **98,** 694–702.
23. Geboes, K., Riddell, R., Öst, A., Jensfelt, B., Persson, T., Löfberg, R. (2000) A reproducible grading scale for histological assessment of inflammation in ulcerative colitis. *Gut* **47,** 404–409.
24. Seldenrijk, C. A., Morson, B. C., Meuwissen, S. G., Schipper, N. W., Lindeman, J., Meijer, C. J. (1991) Histopathological evaluation of colonic mucosal biopsy specimens in chronic inflammatory bowel disease: diagnostic implications. *Gut* **32,** 1514–1520.
25. Krawisz, J. E., Sharon, P., Stenson, W. F. (1984) Quantitative assay for acute intestinal inflammation based on myeloperoxidase activity. Assessment of inflammation in rat and hamster models. *Gastroenterology* **87,** 1344–1350.
26. Klebanoff, S. J., Waltersdorph, A. M., Rosen, H. (1984) Antimicrobial activity of myeloperoxidase. In: *Methods in Enzymology*, Academic Press, New York. *NY* pp. 399–403.
27. Stokes, M. E., Davis, C. S., Koch, G. G. (1995) *Categorical Data Analysis Using the SAS System.* SAS Institute Inc., Cary. NC, 449 pp.
28. Wolfinger, R. D. (1997) An example of using mixed models and PROC MIXED for longitudinal data. *J. Biopharm. Stat.* **7,** 481–500.
29. Forbes, E., Murase, T., Yang, M., Matthaei, K. I., Lee, J. J., Lee, N. A., Foster, P. S., Hogan, S. P. (2004) Immunopathogenesis of experimental ulcerative colitis is mediated by eosinophil peroxidase. *J. Immunol.* **172,** 5664–5675.
30. Talbot, I. C., Price, A. B. (1987) *Biopsy Pathology in Colorectal Disease*. Cambridge University Press, Cambridge, UK.
31. Whitehead, R., Johansen, A., Rubio, C. A. (1995) *Gastrointestinal and Oesophageal Pathology*. Churchill Livingstone. New York, NY.
32. Murthy, S. N., Cooper, H. S., Shim, H., Shah, R. S., Ibrahim, S. A., Sedergran, D. J. (1993) Treatment of dextran sulfate sodium-induced murine colitis by intracolonic cyclosporin. *Dig. Dis. Sci.* **38,** 1722–1734.
33. Murthy, S., Cooper, H. S., Yoshitake, H., Meyer, C., Meyer, C. J., Murthy, N. S. (1999) Combination therapy of pentoxifilline and TNFalpha monoclonal antibody in dextran sulphate-induced mouse colitis. *Aliment. Pharmacol. Ther.* **13,** 251–260.
34. Baert, F. J., D'Haens, G. R., Peeters, M., Hiele, M. I., Schaible, T. F., Shealy, D., Geboes, K., Rutgeerts, P. J. (1999) Tumor necrosis factor alpha antibody (infliximab) therapy profoundly down-regulates the inflammation in Crohn's ileocolitis. *Gastroenterology* **116,** 22–28.
35. D'haens, G.R., Van Deventer, S., Van Hogezand, R., Chalmers, D., Kothe, C., Baert, F., Braakman, T., Schaible, T., Geboes, K., Rutgeerts, P. (1999) Endoscopic and histological healing with infliximab anti-tumor necrosis factor antibodies in Crohn's disease: A European multicenter trial. *Gastroenterology* **116**, 1029-1034.
36. Sandborn, W. J. (2005) New concepts in anti-tumor necrosis factor therapy for inflammatory bowel disease. *Rev. Gastroenterol. Disord.* **5,** 10–18.
37. Hans, W., Schölmerich, J., Gross, V., Falk, W. (2000) Interleukin-12 induced interferon-γ increases inflammation in acute dextran sulfate sodium induced colitis in mice. *Eur. Cytokine Netw.* **11,** 67–74.
38. Kojouharoff, G., Hans, W., Obermeier, F., Mannel, D. N., Andus, T., Schölmerich, J., Gross, V., Falk, W. (1997) Neutralization of tumour necrosis factor (TNF) but not of IL-1 reduces inflammation in chronic dextran sulphate sodium-induced colitis in mice. *Clin. Exp. Immunol.* **107,** 353–358.
39. Woodruff, T. M., Arumugam, T. V., Shiels, I. A., Reid, R. C., Fairlie, D. P., Taylor, S. M. (2003) A potent human C5a receptor antagonist protects against disease pathology in a rat model of inflammatory bowel disease. *J. Immunol.* **171,** 5514–5520.
40. Li, X., Klintman, D., Liu, Q., Sato, T., Jeppsson, B., Thorlacius, H. (2004) Critical role of CXC chemokines in endotoxemic liver injury in mice. *J. Leukoc. Biol.* **75,** 443–452.
41. Zhang, X. W., Liu, Q., Wang, Y., Thorlacius, H. (2001) CXC chemokines, MIP-2 and KC, induce P-selectin-dependent neutrophil rolling and extravascular migration in vivo. *Br. J. Pharmacol.* **133,** 413–421.
42. Godaly, G., Hang, L., Frendéus, B., Svanborg, C. (2000) Transepithelial neutrophil migration is CXCR1 dependent in vitro and is defective in IL-8 receptor knockout mice. *J. Immunol.* **165,** 5287–5294.
43. Smith, M. L., Olson, T. S., Ley, K. (2004) CXCR2 and E-selectin-induced neutrophil arrest during inflammation in vivo. *J. Exp. Med.* **200,** 935–939.
44. Reutershan, J., Morris, M. A., Burcin, T. L., Smith, D. F., Chang, D., Saprito, M. S., Ley, K. (2006) Critical role of endothelial CXCR2 in LPS-induced neutrophil migration into the lung. *J. Clin. Invest.* **116,** 695–702.
45. Williams, E. J., Haque, S., Banks, C., Johnson, P., Sarsfield, P., Sheron, N. (2000) Distribution of the interleukin-8 receptors, CXCR1 and CXCR2, in inflamed gut tissue. *J. Pathol.* **192,** 533–539.